Neck postural stabilization, motion comfort, and impact simulation

Happee, Riender; de Bruijn, E.; Forbes, Patrick; van Drunen, Paul; van Dieën, Jaap H.; van der Helm, Frans

DOI
10.1016/B978-0-12-816713-7.00019-2

Publication date
2019

Document Version
Final published version

Published in
DHM and Posturography

Chapter 19

Neck postural stabilization, motion comfort, and impact simulation

Riender Happee[1], Edo de Bruijn[1,4], Patrick Alan Forbes[2], Paul van Drunen[1,5], Jaap H. van Dieën[3] and Frans Cornelis Theodorus. van der Helm[1]

[1]*Delft University of Technology, Delft, The Netherlands;* [2]*Erasmus Medical Center, Rotterdam, The Netherlands;* [3]*VU Amsterdam, Amsterdam, The Netherlands;* [4]*Medisafe, Bishop's Stortford, United Kingdom;* [5]*Equalis Strategy & Modeling, Utrecht, The Netherlands*

1. Introduction

The human head-neck system is a complex and highly flexible biomechanical structure requiring continuous active stabilization in the presence of gravity. Coordinated feedback control of neck muscle segments is needed to position and stabilize the head in space and to stabilize the individual neck joints in the presence of trunk motion and other perturbations. These are partly conflicting control objectives. In the presence of dynamic trunk motion, for example, while walking or riding a vehicle, it may be beneficial to minimize head rotation and translation in relation to vision and comfort. This can be achieved with a so-called head-in-space control strategy using vestibular and visual feedback. In contrast, humans may use a head-on-trunk control strategy using muscle spindle feedback and cocontraction of antagonist muscles. Such a head-on-trunk control strategy will stiffen the neck, which may not be advantageous in terms of comfort but seems the only strategy that can stabilize individual neck joints and prevent neck buckling.

A range of experimental studies have demonstrated muscle spindle and vestibular afferent feedback contributions to head-neck stabilization through the cervicocollic reflex (CCR) and vestibulocollic reflex (VCR), respectively (Cullen, 2012; Forbes, Dakin, et al., 2013; Goldberg & Cullen, 2011; Keshner, 2009; Keshner, Hain, & Chen, 1999). Peng, Hain, and Peterson (1996) modeled head-neck stabilization in twist and reported CCR and VCR of similar magnitudes. Experimental and modeling studies of the extremities and lumbar spine have shown substantial contributions of cocontraction, where simultaneous activation of antagonist muscles creates an "intrinsic resistance" that can be of a similar magnitude as the "reflexive resistance" (de Vlugt, Schouten, & van der Helm, 2006; Kearney, Stein, & Parameswaran, 1997; Mirbagheri, Barbeau, & Kearney, 2000; van Drunen, Maaswinkel, van der Helm, van Dieën, & Happee, 2013). Keshner (2000) showed a human ability to modulate neck muscle cocontraction, with more cocontraction in elderly subjects.

In section 2 this chapter presents an advanced neuromuscular neck model quantifying the contributions of VCR, CCR, and cocontraction. The model has been presented in detail and validated for anterior−posterior loading (Happee, de Bruijn, Forbes, & van der Helm, 2017) and is extended and validated for other motion directions in this chapter. We present insights into head−neck stabilization and a model that (after further development and validation) can predict head-neck motion in novel conditions.

A wide range of neuromuscular neck models has been presented in the literature ranging from 1-pivot models (Fard, Ishihara, & Inooka, 2003; Peng, Hain, & Peterson, 1997, 1999) to detailed multisegment models (Almeida, Fraga, Silva, & Silva-Carvalho, 2009; Brolin, Hedenstierna, Halldin, Bass, & Alem, 2008; Chancey, Nightingale, Van Ee, Knaub, & Myers, 2003; Hedenstierna, 2008; Meijer et al., 2013; Stemper, Yoganandan, & Pintar, 2004; van Ee et al., 2000; Wittek, Kajzer, & Haug, 2000; Yoganandan, Pintar, & Cusick, 2002) and partial finite element models (Hedenstierna & Halldin, 2008; Hedenstierna, Halldin, & Brolin, 2008; Meyer, Bourdet, Gunzel, & Willinger, 2013; Meyer, Bourdet, Willinger, Legall, & Deck, 2004; Meyer & Willinger, 2009). To study stabilization of individual intervertebral joints, a multisegment model is needed, but we are not aware of any previous multisegment neck model to achieve stabilization in prolonged dynamic loading. Vestibular and visual feedback can separately control head rotation and translation, but we are

DHM and Posturography. https://doi.org/10.1016/B978-0-12-816713-7.00019-2

not aware of any previous neck model to include such separate feedback loops. Hence, we extended a multisegment biomechanical neck model with a new control model addressing the aforementioned limitations (Happee et al., 2017). Contributions of VCR, CCR, and cocontraction were quantified by fitting the model to responses of healthy subjects exposed to trunk perturbations with varying direction and bandwidth, with and without vision.

Insights and models capturing VCR, CCR, and cocontraction can be of value in the medical field for research, diagnosis, and treatment of neck disorders and in fields such as vehicle comfort and impact biomechanics. This chapter elaborates on vehicle motion comfort and impact applications. Motion comfort is addressed by validation in the frequency domain with small loading amplitudes and high bandwidth (see Table 19.1), illustrating the ability of the model to predict head motion in frequency and amplitude ranges relevant for motion comfort. Validation in impact conditions shows that postural control parameters, estimated by fitting the neck model to small-amplitude experimental data, can predict head kinematics in high-amplitude loading conditions reasonably well. For full-body impact simulation, we refer to other chapters in this book.

Paragraph 2 of this chapter focuses on head-neck modeling. Paragraph 3 presents experiments with combined stabilization of the complete spine, in which both trunk and head motions are measured (Fig. 19.1). Models of lumbar spine stabilization are presented with a perspective toward full spine and full-body modeling. Results include analysis of the contribution of feedback and cocontraction in spinal stabilization, in relation to seating conditions, instruction, and presence of vision.

TABLE 19.1 Experimental conditions testing the neck in the frequency domain with subjects restrained on rigid seats.

Short name	Seat motion	Bandwidth [Hz]	Vision and instruction sets	References
APEO APEC	Anterior-posterior (AP) translation	0.2–4	EO = Eyes open, instructed to focus at a marker in front EC = Blindfolded, instructed to maintain a comfortable upright seating position. In both conditions, subjects listened to a science-based radio program to distract them from the stabilization process and minimize voluntary responses.	Forbes, de Bruijn et al. (2013)
LatEC	Lateral (LAT) translation	0.15–4	EC = Blindfolded, instructed to maintain a comfortable upright seating position. Subjects listened to a science-based radio program to distract them from the stabilization process and minimize voluntary responses.	Forbes (2014)
RollEC	Roll lateral rotation	0.15–4		
PitchVS PitchNV PitchMA	Pitch anterior/posterior rotation	0.35–3.05	VS = Voluntary stabilization "required that the subject keep the head-referenced light signal coincident with a stationary target spot" (using a head-mounted light spot) NV = No vision "in the dark, the subject was given the task of stabilizing the head by imagining the stationary target spot and the head-referenced light signal" MA = Mental arithmetic; "a mental calculation task was provided so that the subject's attention was removed from the task of stabilization while rotation in the dark was ongoing.	Keshner, Cromwell, and Peterson (1995)
TwistVS TwistNV TwistMA	Twist left/right neck axial rotation	0.185–4.11		Stensdotter et al. (2016)
	Anterior-posterior translation	1–16	Corridors derived from multiple studies with various conditions with rigid seats with back support	Paddan and Griffin (1998)
	Lateral translation	1–14		
	Vertical translation	1–30		
	Vertical translation	0–25	Rigid seat with back support, subjects looked horizontally at a cross approximately 1.3 m away on a wall moving with the vibration table	Paddan and Griffin (1988)

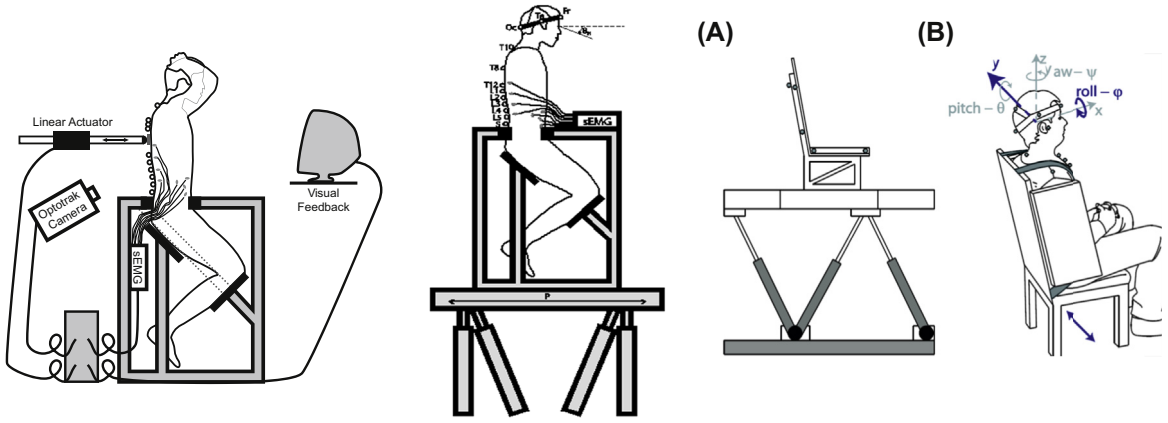

Thorax pushing machine to test lumbar stabilization with the pelvis clamped (van Dieën, van Drunen, & Happee, 2017; van Drunen et al., 2013)

6DOF motion platform tests of lumbar and neck stabilization with the pelvis clamped (van Drunen, Koumans, van der Helm, van Dieën, & Happee, 2015; van Drunen, van der Helm, van Dieën, & Happee, 2016)

6DOF motion platform tests of neck stabilization with rigid seat and 5 point harness belt, and with cushioned lateral arm support in case of lateral loading (Forbes, 2014; Forbes, de Bruijn, Schouten, van der Helm, & Happee, 2013)

FIGURE 19.1 Experimental setups investigating stabilization of the lumbar and cervical spine; in all studies, 3D motion was recorded using optical markers.

1.1 Comfort of automated driving

As outlined in this paragraph, knowledge and models of postural stabilization and the resulting head motion are essential in the domain of motion comfort, particularly in self-driving vehicles. In automated vehicles, we may use the travel time for work or leisure activities (Kyriakidis, Happee, & De Winter 2015), but this requires high comfort levels, where self-driving car sickness is a particular concern (Diels & Bos, 2016). Hence we need to carefully design the "driving style" of automated vehicles (Bellem, Schönenberg, Krems, & Schrauf, 2016). An aggressive driving style adopted by automated vehicles will result in excessive body motion, leading to discomfort and hampered performance in work or leisure activities. A short track study indicated that in automated driving with eyes off road, drivers preferred lower acceleration levels in an automated lane change than during manual driving (Lange et al., 2014). Festner, Baumann, and Schramm (2016) showed significantly improved comfort, perceived safety, and general well-being when reducing jerk from 2.9 to 1.3 m/s^3 while maintaining peak accelerations around 1.8 m/s^2 in braking from 120 km/h to 80 km/h in an automated vehicle on a test track. In this study, no effect of task on perceived comfort was found comparing road monitoring, reading, and writing numbers. Passive and active suspension systems can attenuate road-induced disturbances (Shyrokau, Wang, Savitski, Hoepping, & Ivanov, 2015), and active roll suspension control can attenuate horizontal body forces and reduce postural disturbances (Bär, 2014). In designing such active suspensions, the effects on 3D head motion must be taken into account.

Motion sickness and (dis)comfort are influenced by the exposure to mechanical and visual motion cues, as well as any disparity between them. Motion sickness is primarily caused by motion frequencies below 0.5 Hz while frequencies above 0.5 Hz can elicit general vibration discomfort (ISO-2631-1, 1997). The act of driving makes drivers virtually insensitive to motion sickness, whereas passengers typically suffer more, especially when deprived of visual information about self-motion obtained from views out of the window (Diels & Bos, 2016). Current standards assess the overall vibration discomfort of seated people by summation of frequency-weighted accelerations at the seat, the back, and the feet (British Standards Institution, 1987; ISO-2631-1, 1997). While accelerations at the seat, the back and the feet have been shown to relate to comfort, it is widely accepted that head motion, as perceived by the vestibular organ and vision, is a key determinant of (dis)comfort and motion sickness (Bertolini & Straumann, 2016). Thus, the "seat-to-head transmissibility" (STHT) must be taken into account to assess vestibular and visual contributions to motion perception and comfort. This chapter presents experimental and modeling efforts to investigate and predict STHT. Finally, an outlook will be given on using biomechanical models to investigate and enhance motion comfort of automated driving.

2. Neck modeling

2.1 Biomechanical head–neck model

Happee et al. (2017) presented a multisegment cervical spine model with postural stabilization through VCR and CCR loops and cocontraction. A 3D multisegment nonlinear neck model (de Bruijn, van der Helm, & Happee, 2015; de Jager, 1996; van der Horst, 2002) was adopted. The model was extended with postural control (Fig. 19.2), stabilizing the head-neck system in the presence of gravity and trunk motion and realistically capturing head translation and rotation. The model contains nine rigid bodies representing the head, seven cervical vertebrae (C1–C7), and the first thoracic vertebra (T1). The eight intervertebral joints allow 3D rotational and translational motion, resulting in a total of 48 degrees of freedom (DOF). Muscles (34 muscles, totaling 129 elements per body side) were implemented as line elements based on dissection of a single specimen (Borst, Forbes, Happee, & Veeger, 2011) with 'via points' connecting muscles to adjacent vertebrae to ensure the muscles take on a curved path during head-neck displacement and with nonlinear Hill-type contractile elastic and series elastic dynamics. Gravity is simulated as a 9.81 m/s^2 gravitational field acting on the skull and the vertebrae.

The neck model was validated in passive bending and twist and in isometric loading where the ligamentous spine stiffness, instantaneous joint centers of rotation, muscle moment arms, cervical isometric strength, and muscle activation patterns were in general agreement with biomechanical data (de Bruijn et al., 2015). The control model, parameter estimation, and validation in anterior–posterior loading can be found in the article by Happee et al. (2017). For this chapter, VCR feedback loops were added for head lateral motion and twist. The lateral loops are equivalent to the anterior–posterior loops and provide feedback of head roll angular velocity (G_{sclat}), roll angle (G_{tonlat}), and lateral acceleration ($G_{phaslat}$) in space. The head twist feedback loops provide feedback of head twist angular velocity ($G_{sctwist}$) and twist angle ($G_{tontwist}$) in space. Here it shall be noted that the VCR can differentiate static head pitch and roll from graviception, whereas static twist can only be estimated through integration of perceived rotational velocity and will hence be imprecise. However, head rotation in all directions can be perceived visually. The current model combines vestibular and visual feedback of head motion in space in one loop, which will be detailed in future model versions. The biomechanical neck model was implemented in the simulation software MADYMO 7.5 (MADYMO, 2012). Sensor dynamics, neuromuscular control, delays, and muscle dynamics were implemented in MATLAB R2012b (Mathworks, 2012). Euler integration was applied with a fixed time step, which was generally set to 40 μs, resulting in a computation time of

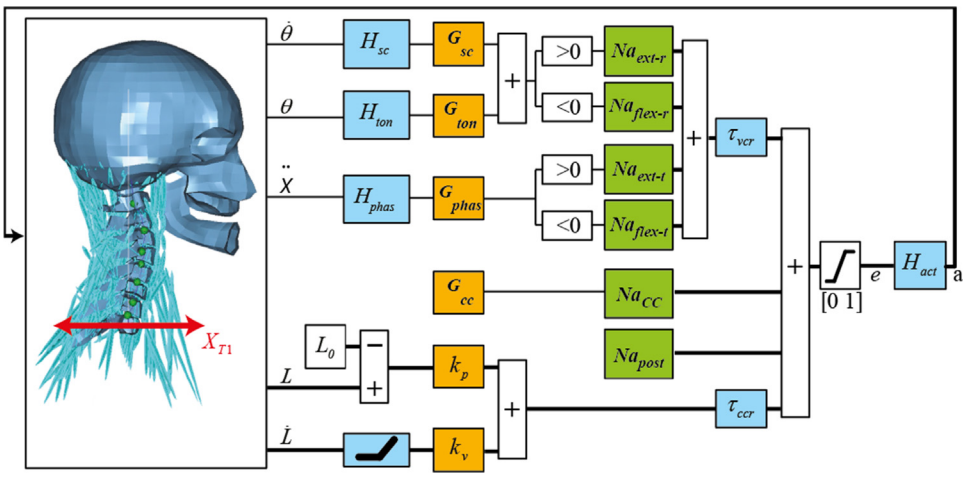

FIGURE 19.2 Neural control model of the neck. Blue blocks (gray blocks in print version) contain sensory and muscle activation dynamics and delays and orange blocks contain the feedback sensitivity (gain) and cocontraction parameters. Green blocks (light gray blocks in print version) are muscle synergy vectors converting scalar control signals to an appropriate activation of multiple muscle segments for flexion (Na_{flex-r} for rotation, Na_{flex-t} for translation), extension (Na_{ext-r} for rotation, Na_{ext-t} for translation), cocontraction (Na_{cc}), and postural activity counteracting gravity (Na_{post}). The VCR provides feedback of head angular velocity θ', angle θ, and acceleration X'' with sensor dynamics H_{sc}, H_{ton}, H_{phas}, and feedback sensitivity parameters G_{sc}, G_{ton}, G_{phas}. The CCR provides feedback of muscle contractile element (CE) length "L" with sensitivity parameter k_p and velocity L' with sensitivity parameter k_v where muscle CE reference length L_0 represents the desired posture. Neural pathway delays are defined for VCR (τ_{vcr}) and CCR (τ_{ccr}). H_{act} captures muscular activation dynamics, transforming neural excitation (e) into muscle active state (a). X_{T1} is the applied mechanical perturbation being translation and/or rotation of the base of the neck. Thick lines indicate multiple signals for all 258 muscle segments. This figure shows anterior–posterior control. Equivalent VCR loops have been added for lateral and twist control as described in the text. *CCR*, cervicocollic reflex; *VCR*, vestibulocollic reflex.

roughly 130 times real time on a 2.8-GHz processor. In the high-severity (15G) impact simulation, the time step was reduced to 10 μs to achieve stable and accurate results.

2.2 Validation in the frequency domain

The neck model was validated using biomechanical data from six studies as summarized in Table 19.1. In all experiments, healthy adult human subjects were restrained by a harness on a rigid seat mounted on a motion platform. In the lateral (LAT) tests, the subjects were laterally supported with adaptable cushioned plates (Forbes, 2014) (Fig. 19.1). In the anterior−posterior (AP) tests, the T1 translation (base of the neck) was recorded and applied as input to the neck model and used to derive transfer functions from torso motion to head motion. For the other tests, torso motion was reported to be close to the seat motion, and the seat motion was applied to T1 in the neck model. Checking the transmission from seat motion to T1 in own data (Forbes, 2014; Forbes, de Bruijn et al., 2013), we indeed found gains close to one for torso horizontal translation and roll, but we also found some phase shifts and therefore do not report phase in the following figures. For the twist conditions, we used data from the work of Stensdotter, Dinhoffpedersen, Meisingset, Vasseljen, and Stavdahl (2016), who repeated experiments performed by Keshner and Peterson (1995). The new data set was selected as it includes more subjects (17 instead of 7) and describes head global motion as a function of torso motion recorded at T2. To extend the validation to higher frequencies, data for seat translation in three directions were adopted from a review on STHT (Paddan & Griffin, 1998). One specific data set for vertical loading (Paddan & Griffin, 1988) contained in this review was also adopted as it includes relevant interaction response data for head AP and pitch motion.

2.2.1 Validation results

For each condition, the VCR and CCR gains and cocontraction were estimated by fitting the model to the experimental data. For vertical loading, the data were not very informative, and we applied three parameter sets estimated for horizontal seat translation and for seat rotation, discussed elsewhere in the chapter. Parameters and model fits in time and frequency domain for AP loading with eyes open and eyes closed up to 8 Hz can be found in the study by Happee et al. (2017). The vestibular loops were needed to fit the experimental results in particular with rotational perturbations. Muscle feedback was needed to stabilize the individual neck joints and prevent anterior-posterior neck buckling (Happee et al., 2017). Cocontraction was estimated to be at most 1%.

Figs. 19.3 and 19.8 show validation results in the frequency domain for the six seat motion directions. To extrapolate and interpolate results, the same parameter sets were simulated with a 0.1−40 Hz perturbation with similar power. In each figure, the head response is shown for the perturbed seat motion direction as well as the main interaction terms. Fig. 19.3, for instance, shows relevant head pitch motion in response to AP seat translation. Fig. 19.4 shows head roll and twist in response to lateral seat translation.

In most cases, the model fits the data well, taking into account the spread found between and within experiments. In AP loading (Fig. 19.3), the model fits our own data well and thereby shows lower gains at high frequency than the gray corridor from the review by Paddan and Griffin (1998). In unpublished experiments, we explored effects of instructions to relax, to resist, and to raise the muscular activation level using visual feedback of muscular activity (EMG). In this unpublished data set, the instruction to relax yielded responses similar to the current data (line APECexp), while the resist and EMG feedback elicited gain peaks above two around 4 Hz, similar to the corridor from the study of Paddan and Griffin (1998), suggesting such peaks to derive from resist strategies and raised cocontraction levels. With vertical loading, the model response shows amplification peaks above 8 Hz where the experimental corridors peak between 3 and 8 Hz (Fig. 19.5). This is presumably due to the dynamic vertical response of the lumbar and thoracic spine and may be addressed by integrating the neck model in a full-body human model. In the roll experiment, the model adequately captured head roll and twist (Fig. 19.6). The model overestimated head lateral translation above 2 Hz, but the actual translation at these frequencies was small. Three instruction sets were evaluated with seat pitch (Fig. 19.7) and twist (Fig. 19.8) rotations. Instruction sets where subjects actively control head rotation with visual feedback and without visual feedback (NV) required high VCR feedback gains G_{ton} for head orientation in space. Thus, the model accurately captures the experimentally observed head-in-space control strategy at low frequencies with seat pitch and twist perturbations.

2.2.2 Six Degrees of Freedom neck dynamics

The aforementioned results show model fits for head motion in the applied seat motion direction and several other (interacting) head DOF. Available data sets were limited in bandwidth, but the model allows us to extrapolate the human response to a larger frequency range. Fig. 19.9 shows such results for all six seat perturbation and head response directions.

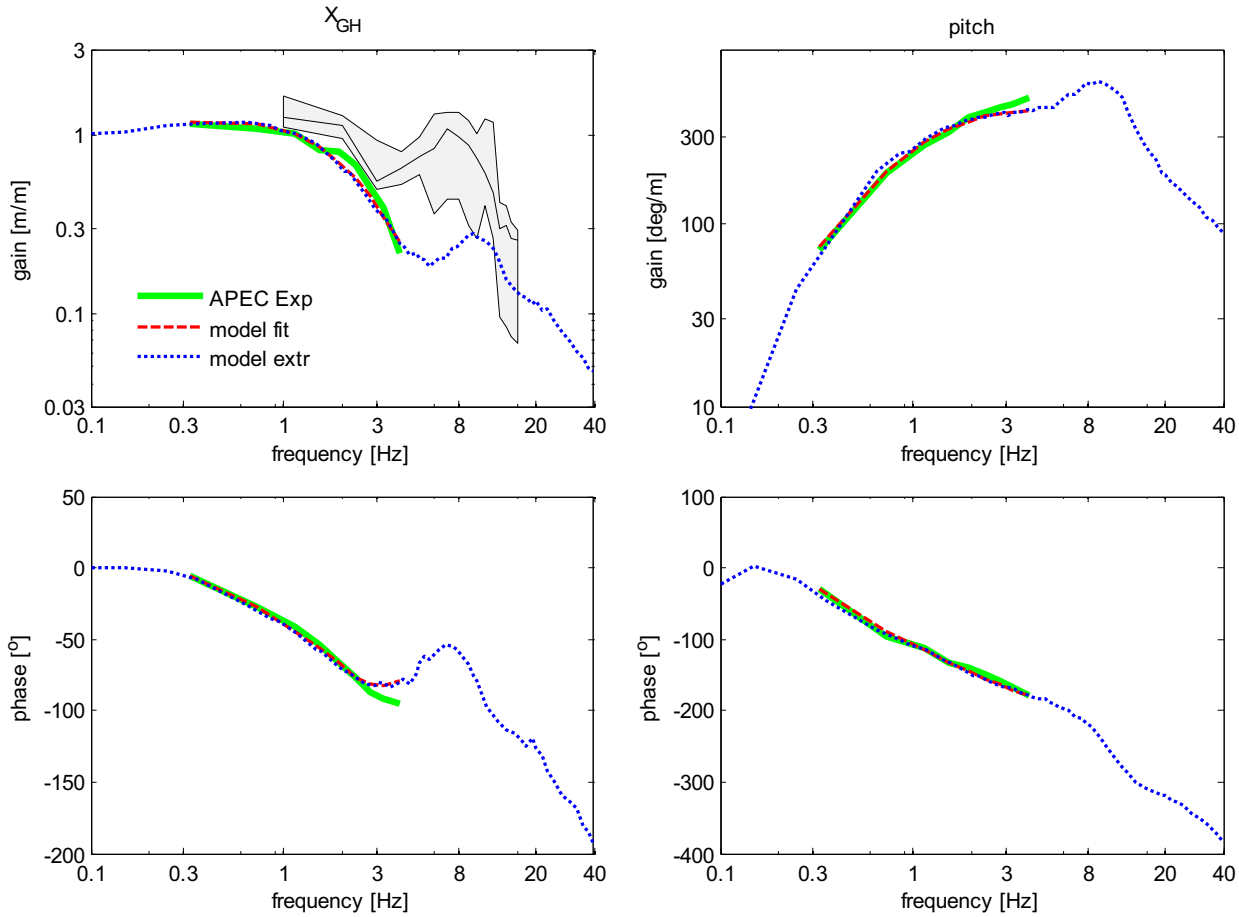

FIGURE 19.3 Neck model validation for anterior–posterior seat translation with eyes closed (APEC). The red line (dark gray line in print version) describes the model fit, and the blue line (black line in print version) extrapolates this simulating a 0.1–40 Hz perturbation with similar power. The gray corridor shows mean and interquartile ranges over studies reviewed by Paddan and Griffin (1998).

In all cases, the "seat" motion was applied directly at T1. Three parameter sets were simulated combining parameters estimated for different conditions (see Table 19.1) in terms of applied seat motion, visual feedback, and instructions:

1. Trans combines parameters for AP and lateral seat translational motion with eyes closed (APEC & LatEC);
2. RotVS combines parameters for pitch and twist seat rotation with visual voluntary stabilization of head rotation in space (PitchVS & TwistVS);
3. RotMA combines parameters for pitch and twist seat rotation in the dark with mental arithmetic (PitchMA & TwistMA).

As the model and the adopted posture are left–right symmetric, several interaction terms in Fig. 19.9 are zero; for instance, AP motion (top row) does not induce lateral, roll, and twist motion. Other interactions show zero gains as the linearized transmission is zero, but nonlinear behavior will induce higher harmonics. For instance, lateral seat motion (second row) will induce some vertical head motion, but this will be identical for left or right seat motion, leading to a zero linearized transmission.

Fig. 19.9 shows that T1 translation induces head motion in the corresponding direction with a gain close to one at low frequencies. At mid-frequencies, some amplification (gain>1) is shown for all three translation motion directions in particular with the more active control set RotVS. The control strategy Trans more effectively reduces head translations, and the strategy RotVS very strongly reduces head rotations up to around 1 Hz. These head rotations will be particularly relevant in their effect on motion comfort and sickness (Bertolini & Straumann, 2016). Given these apparent effects of motion direction, visual feedback, and instruction, it will be important to assess postural control strategies in the conditions of interest. For driving comfort, these should include real vehicles in realistic driving conditions, with and without vehicle automation and eyes on road as well as eyes off road performing nondriving tasks.

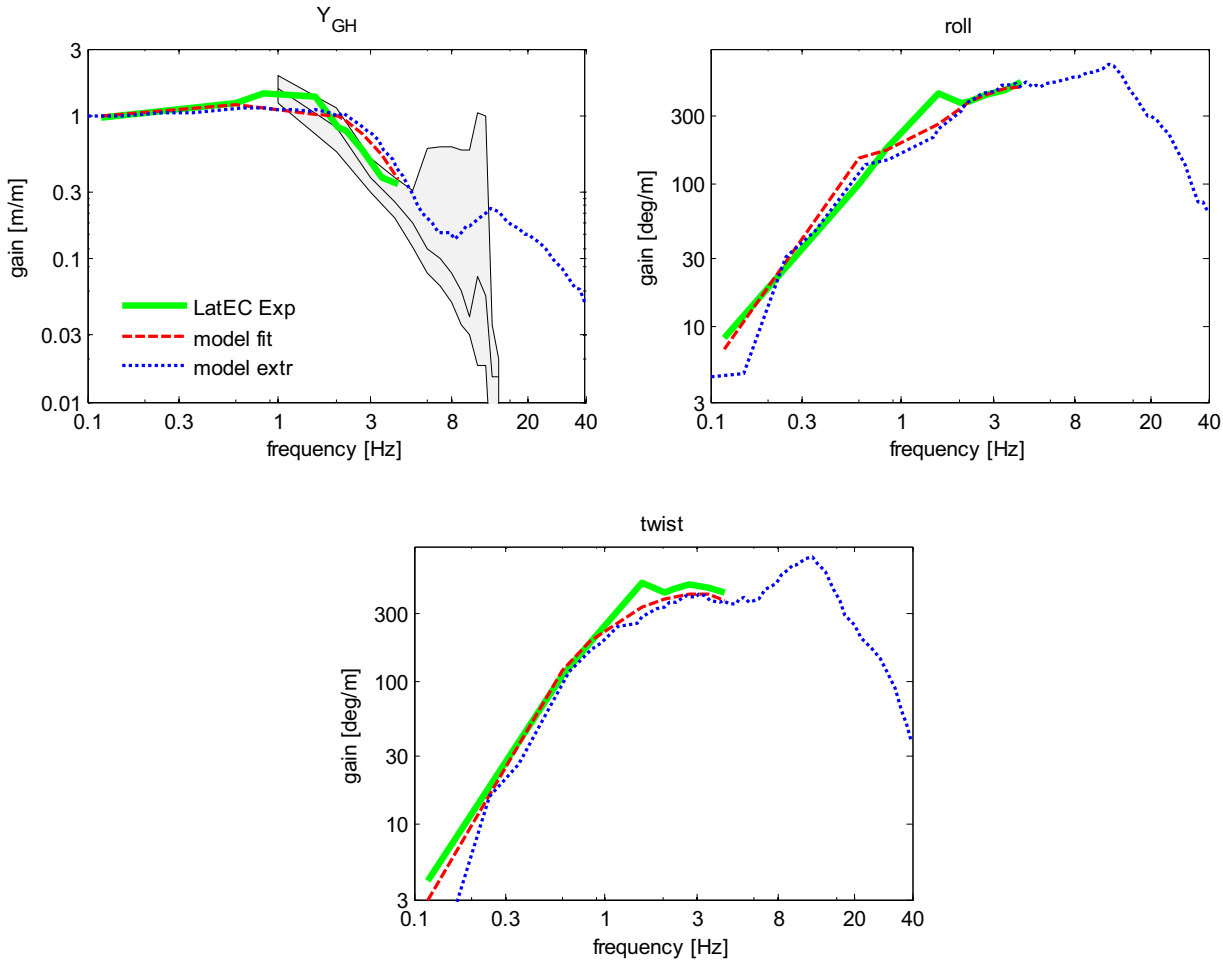

FIGURE 19.4 Neck model validation for lateral seat translation with eyes closed (LatEC). The red line (dark gray line in print version) describes the model fit, and the blue line (black line in print version) extrapolates this simulating a 0.1−40 Hz perturbation with similar power. The gray corridor shows mean and interquartile ranges over studies reviewed by Paddan and Griffin (1998).

2.3 Validation for impact conditions

Volunteer data were used as collected at the Naval Biodynamics Laboratory (NBDL) in the US (Ewing et al., 1976; Ewing & Thomas, 1972; Ewing, Thomas, Patrick, Beeler, & Smith, 1969). Volunteers (young and well-trained marines) were seated in an upright position on a rigid seat mounted on a sled and exposed to short-duration accelerations simulating frontal impacts. Clusters of accelerometers and photographic targets were mounted to the subject, to monitor 3D motions of the head and T1 (Fig. 19.10). The subjects were restrained by shoulder straps, a lap belt, and an inverted V-pelvic strap tied to the lap belt. Upper arm and wrist restraints were used to prevent flailing. The volunteers were asked to take a normal automotive posture. The initial head angle was 0°, where the head angle was defined as the angle between the Frankfort plane and the horizontal plane. The Frankfort plane is defined as the imaginary plane passing through the external ear canals and across the top of the lower bone of the eye sockets.

We used the frontal impact loading set with 15G peak sled acceleration. To our knowledge, this is the most severe frontal volunteer test instrumented such that it is suitable for validation (van der Horst, 2002; van der Horst, Thunnissen, Happee, & van Haaster, 1997). We also simulated comparable tests with 10G and 3G peak sled acceleration. In the 15G condition, the T1 AP acceleration as measured with the T1 bracket was available and used as input to the neck model. In the 10G and 3G conditions, T1 data were not available, and the measured seat acceleration was applied to T1 in the model, leading to some timing mismatch in 10G and 3G conditions.

For the validation, we adopted neck postural control parameters estimated for AP tests with a low bandwidth of 0.3−1.2 Hz, with eyes open (condition B1EO in the work of Happee et al. (2017)). The low bandwidth was seen as most

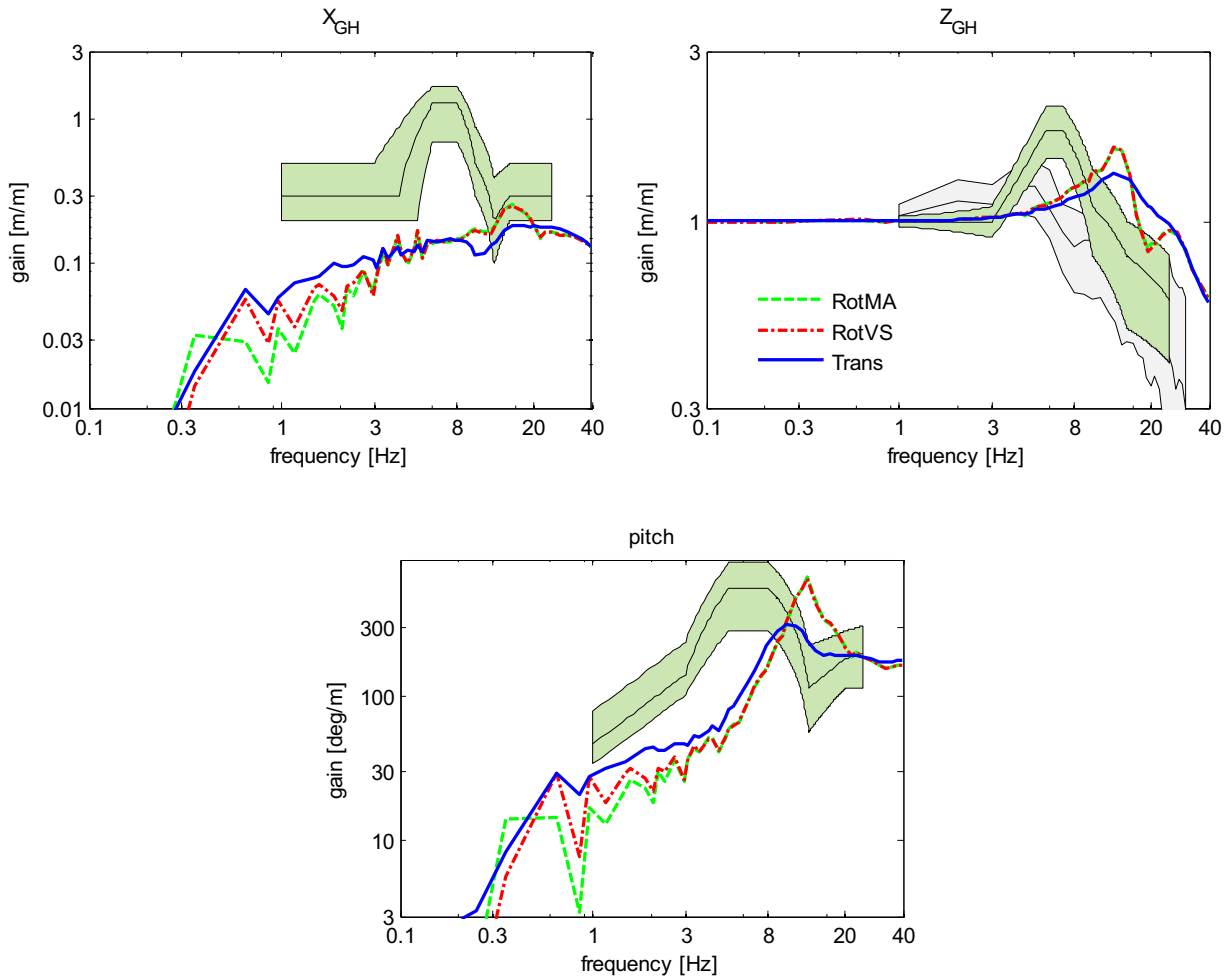

FIGURE 19.5 Neck model validation for vertical seat translation. The three lines describe the model response using parameters estimated for AP and lateral translational perturbations (Trans), for pitch and twist with visual voluntary stabilization (RotVS), and for pitch and twist in the dark with mental arithmetic (RotMA). The gray corridor shows mean and interquartile ranges over studies reviewed by Paddan and Griffin (1998). The green corridor is based on Paddan and Griffin (1988).

representative for the case studied, which includes mainly low-frequency motion. We also simulated a passive response without VCR and CCR (Fig. 19.11). Apparently in all three conditions, reflexive muscle activation has a substantial effect on head motion. Reflexive stabilization limits the peak head rotation angles and gradually restores the initial posture. The passive model shows a strong rebound and finally settles with around 40° flexion.

This validation shows that postural control parameters estimated fitting the model to small-amplitude experimental data can reasonably well-predict postural responses in high-amplitude loading conditions. Head rotation and head resultant linear acceleration adequately match the volunteer corridors where the timing mismatch at 3 and 10 G can be explained by the applied T1 motion as described previously. Head rotational acceleration shows notable deviations. It must be stated that the parameters were estimated with a different set of subjects and a different seat and belt layout than those in the impact tests. Ideally tests with low and high amplitude will be combined using the same setup and subjects for further validation (Happee, de Vlugt, and van Vliet (2014) for such tests at the arm). The passive properties of the joint structures are implemented using nonlinear functions including stiffening at larger deformations. These nonlinear passive properties are essential for high-severity loading conditions (van der Horst, 2002; van der Horst, Bovendeerd, Happee, & Wismans, 2001; van der Horst et al., 1997). The implemented sensory dynamics and feedback loops are linear. Apparently, a nonlinear biomechanical model with linear feedback provides reasonable results.

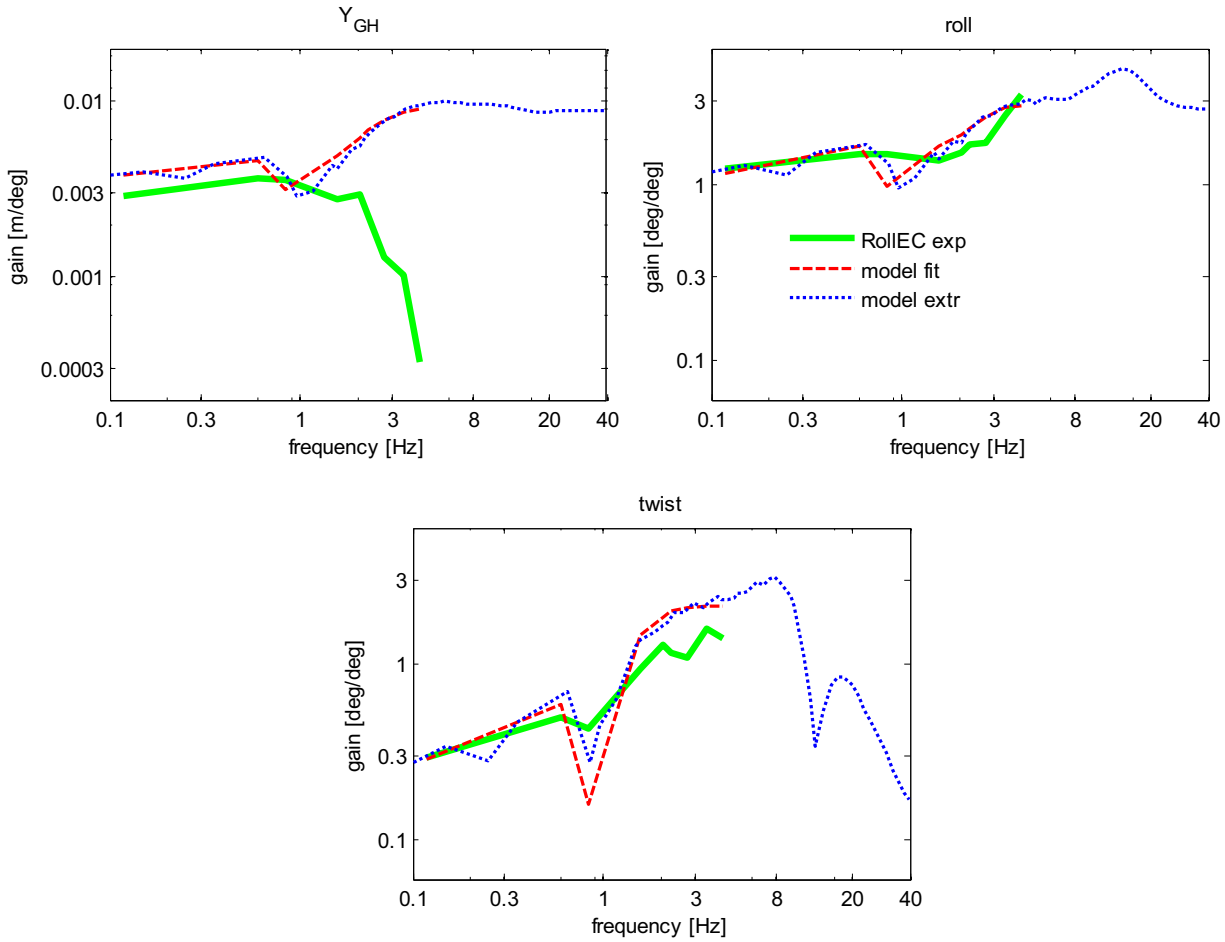

FIGURE 19.6 Neck model validation for lateral seat rotation with eyes closed (RollEC). The red line (dark gary line in print version) describes the model fit, and the blue line (black line in print version) extrapolates this simulating a 0.1−40 Hz perturbation with similar power.

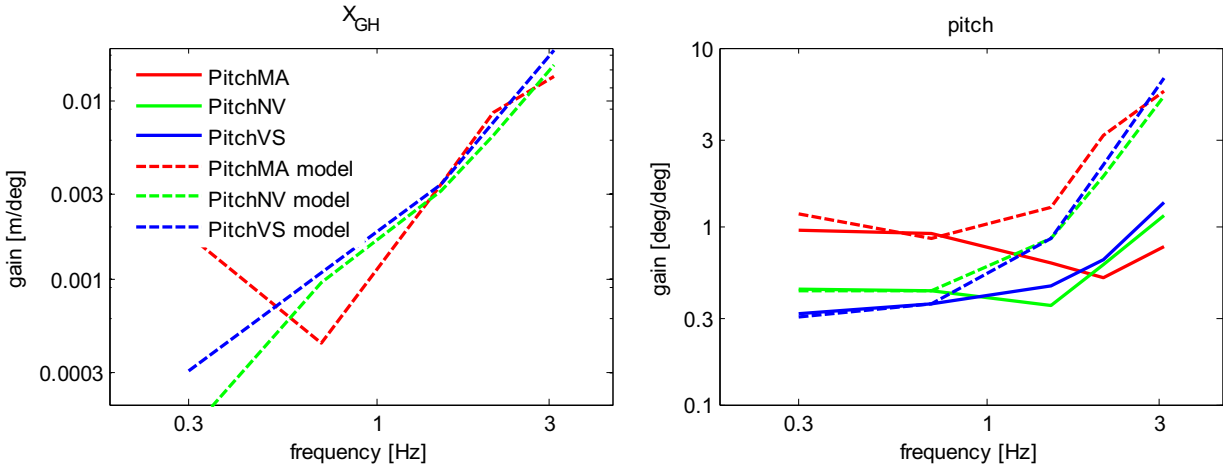

FIGURE 19.7 Neck model validation for anterior-posterior seat rotation (PitchMA, PitchNV, PitchVS).

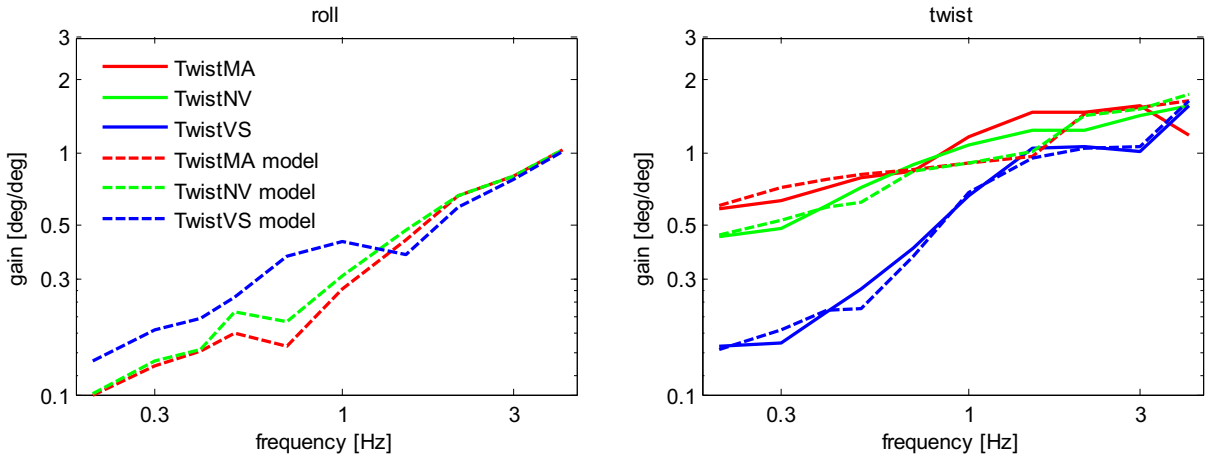

FIGURE 19.8 Neck model validation for left–right axial seat rotation (TwistMA, TwistNV, TwistVS).

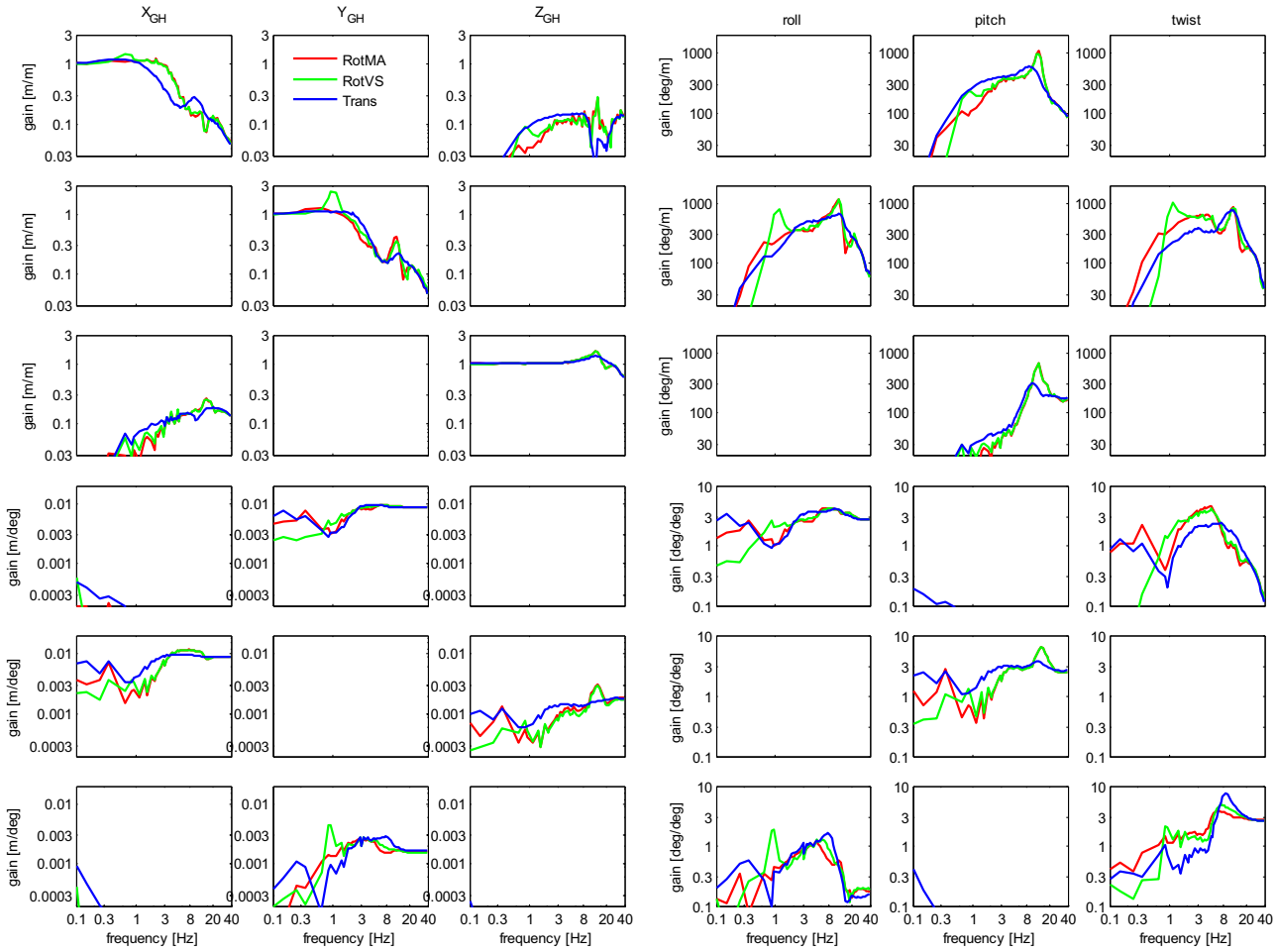

FIGURE 19.9 Six degrees of freedom head–neck model response. Rows describe applied T1 motion conditions with, from top to bottom: AP, lateral and vertical translations, roll, pitch, and twist rotations. Columns describe the corresponding head motions. The three lines describe responses using parameter sets estimated for AP and lateral translational motion (Trans), for pitch and twist with visual voluntary stabilization (RotVS), and for pitch and twist in the dark with mental arithmetic (RotMA).

FIGURE 19.10 NBDL volunteer test configuration, instrumentation (left), posture at pulse onset (mid), and posture at maximum head rotation with 15G loading (right). *NBDL*, Naval Biodynamics Laboratory.

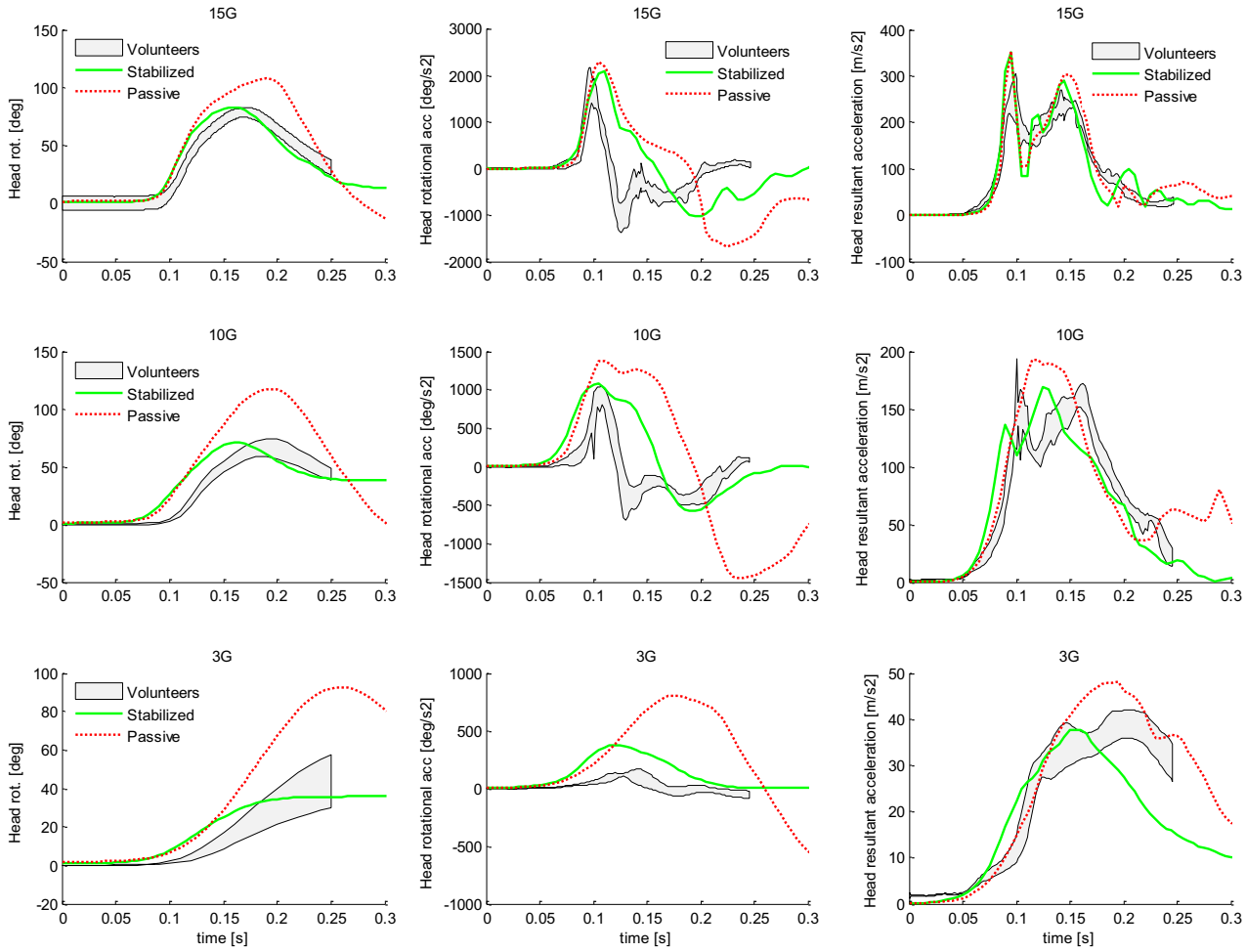

FIGURE 19.11 Validation for impact conditions using NBDL forward flexion volunteer loading with 15G (upper), 10G (mid), and 3G (bottom) peak rearward seat acceleration, stabilized with VCR and CCR (green [light gray in print version]) and passive (red [dark gray in print version]). Volunteer response corridors are shown in gray. *CCR*, cervicocollic reflex; *NBDL*, Naval Biodynamics Laboratory; *VCR*, vestibulocollic reflex.

3. Lumbar spine and neck modeling

The lumbar spine and neck are the most flexible sections of the human spine. In erect postures, lumbar stabilization determines trunk motion and thereby affects head−neck stabilization. Full-body human models including multisegment models of the complete spine have been developed and validated for impact loading (Happee, Hoofman, van den Kroonenberg, Morsink, & Wismans, 1998; Happee, Verver, & de Lange, 2000; Meijer et al., 2013; Östh, Brolin, & Bråse, 2015; Östh, Eliasson, Happee, & Brolin, 2014; Östh, Mendoza-Vazquez, Svensson, Linder, & Brolin, 2016). Such models have also been validated for vertical vibration transmission on rigid and compliant seats (Happee et al., 2000; Verver,

Dalenoort, & Mooi, 2005) but remain to be validated for vibration transmission in other loading directions. Lumped mass and finite element models of the pelvis and lumbar region have been developed as well but require further integration and validation for the simulation of vibration loading in full-body seat to human interaction. Therefore, this paragraph focuses on simplified models of lumbar bending and presents experimental results including trunk and head motion.

Two experimental setups have been used to assess lumbar stabilization in the anterior-posterior direction (Fig. 19.1). With the thorax pushing machine, subjects were perturbed at the back. With the 6DOF platform, pelvic perturbations were applied with the upper body free. The pushing machine mimics upper body loads during daily life activities involving, for instance, arm and/or head movements. The platform motions mimic lower body motions as occurring in various types of vehicles and in walking. In both setups, we measured trunk kinematics and lumbar muscular activity (EMG), while subjects assumed a kneeling-seated posture supported at feet and knees. The pelvis was clamped between cushioned plates to minimize (but not fully eliminate) pelvic rotation and translation.

The thorax pushing machine applied continuous time-varying forces at the back at the height of T10 with a 60 N preload up to 15 Hz. In this setup, trunk kinematics were described in terms of translations instead of rotations (Fig. 19.12) as the necessary effective rotation point was not well defined and inconsistent over subjects and tasks. Using the displacement and EMG, a lumbar stabilization model was developed uniquely, separating stabilizing contributions of intrinsic stiffness and damping (cocontraction) and muscle (spindle) feedback (length and velocity). This model adequately captured the trunk kinematic response (Fig. 19.12) as well as the EMG up to 4 Hz (van Drunen, Maaswinkel, van der Helm, van Dieën, & Happee, 2014). Using a larger data set, it was found that including muscle acceleration feedback enhanced the fit, in particular, for the EMG (van Dieën, van Drunen, & Happee, 2017).

The model allowed us to estimate the relative contributions of intrinsic and reflexive stabilization to low-back stabilization during trunk perturbations and showed that intrinsic contributions are similar to or larger than reflexive contributions. Varying the instructions from 'relax' to 'resist the perturbations' showed a 61% reduced displacement realized by significantly higher intrinsic stiffness and position and velocity feedback. Tests on the 6DOF moving platform allowed further exploration of spinal stabilization applying pelvic perturbations. Experiments with vision showed a modest reduction of trunk and head rotation compared to blindfolded conditions both with platform translation (van Drunen, Koumans, van der Helm, van Dieën, & Happee, 2015) and rotation experiments (van Drunen, van der Helm, van Dieën, & Happee, 2016). Platform translations resulted in similar trunk dynamic responses as in the trunk perturbation setup. We found that a rotation point between the lumbar vertebrae L4 and L5 adequately captured lumbar bending up to 5 Hz during pelvic anterior-posterior translations. Therefore, a one-pivot model was developed describing lumbar anterior−posterior bending in terms of angles and torques (van Drunen et al., 2015). Again the model indicated intrinsic contributions of similar magnitude as reflexive contributions, but now velocity feedback exceeded intrinsic damping, while intrinsic stiffness exceeded position feedback (Fig. 8 in van Drunen et al. (2014)). In an exploratory analysis, a visual feedback loop with a long-latency (250 ms) torso angular feedback was included in the model, which somewhat improved the fit of kinematics and EMG.

In this experiment, we captured both trunk and head kinematics. Trunk translations (X_{GT}) were close to platform translations in particular with the resist instruction (Fig. 19.13, *left*). Head translations (X_{GH}) exceeded trunk translations (X_{GT}) up to 3 Hz (Fig. 19.13—*middle* vs. *left*). Surprisingly, head rotations were only ~2% of torso rotations (Fig. 19.13—*right*).

Platform anterior−posterior (pitch) rotation experiments elicited new insights into lumbar and cervical stabilization (van Drunen et al., 2016). Upon rotating the platform around the estimated lumbar rotation center between L4 and L5, we expected a vestibular and visual control strategy effectively stabilizing the trunk in space. However, with a neutral instruction (balance naturally), torso rotations exceeded the platform rotations over the entire tested frequency range of

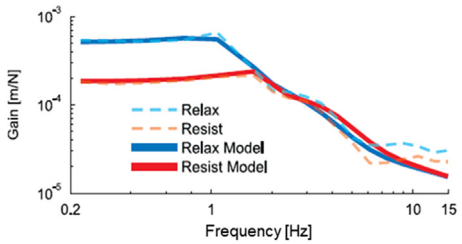

FIGURE 19.12 Lumbar spine model validation with anterior-posterior translation loading with thorax pushing machine; the gain describes torso displacement as a function of applied force at the back.

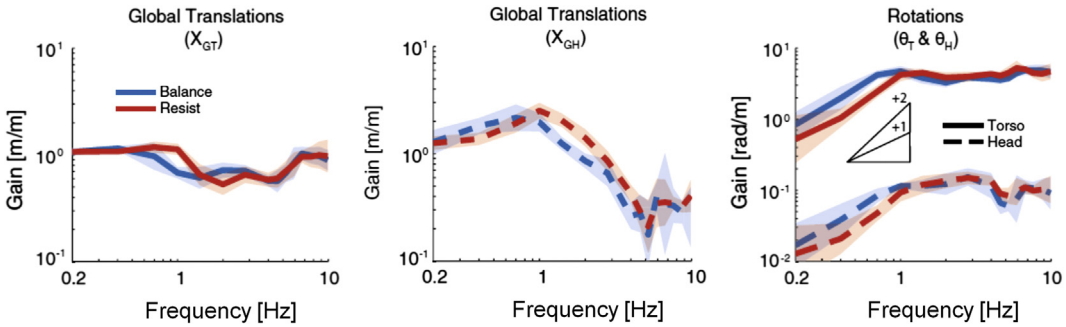

FIGURE 19.13 Torso anterior–posterior translation (left), head translation (mid), and torso and head rotation (right) in response to platform anterior–posterior translation with a neutral instruction (balance naturally) or minimize flexion/extension excursions (resist) with eyes closed.

0.2–10 Hz. Only with an explicit instruction to "minimize sway," a trunk in space control strategy did appear. However this was not fully effective as substantial torso rotations remained (~50% of platform rotations below 0.8 Hz, see Fig. 19.14). Without vestibular and visual feedback, torso rotations at low frequency would have exceeded platform rotations (gains above one) due to the destabilizing effects of gravity. Cocontraction and muscle feedback could stiffen the spine and thereby reduce torso rotation relative to the pelvis, but this could not explain gains below one for the transmission of pelvis to torso rotation. In particular, vestibular feedback contributed to trunk in space stabilization because results with eyes-closed conditions showed only a slight increase in torso rotations. In contrast to the large torso rotations found, head rotations were (similar to the translational experiments) only ~2% of trunk rotations. Apparently, in this configuration, with a clamped pelvis on a rotating platform, subjects were not well able to dynamically counteract the destabilizing effect of gravity on the trunk but could well stabilize head orientation in space.

4. Discussion

4.1 Insights gained in neck postural stabilization

A detailed multisegment neck model has been developed including vestibular/visual and muscular feedback loops and cocontraction. The VCR contributed to head-in-space stabilization with a strong reduction of head rotation with anterior–posterior (AP) seat translation (Happee et al., 2017). Similar effects were observed with lateral seat translation. Not surprisingly, the VCR contribution to minimize head rotation in space was even larger in conditions with seat rotation, where the VCR has to overcome the resistance offered by the CCR, cocontraction, and passive structures. In particular conditions with axial seat rotation, where subjects were instructed to minimize head rotation in space with eyes closed (TwistNV) and eyes open (TwistVS) could only be reproduced using two VCR rotational loops: G_{sc} providing feedback of head rotation velocity as sensed by the semicircular organs using vestibular sensitivity functions (Fernandez, Goldberg, & Abend, 1972; Schneider, Jamali, Carriot, Chacron, & Cullen, 2015) and a second loop G_{ton} representing feedback of the head rotation angle. The first loop (G_{sc}) controls mid-frequencies, whereas the second loop (G_{ton}) controls low frequencies. In the current model, this second loop assumes perfect knowledge of head rotation in space. This can be obtained from integration of rotational velocity as sensed by the semicircular organ, from graviception by the otoliths and from visual

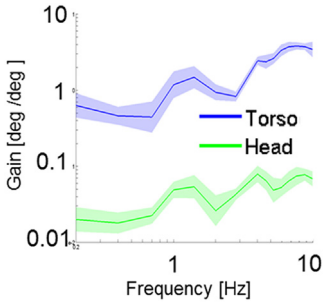

FIGURE 19.14 Torso and head anterior rotation in response to platform anterior rotation with an explicit instruction to "minimize sway" with eyes open.

information. The current model combines vestibular and visual feedback of head motion in space. Further experiments and modeling efforts will aim to capture sensory integration of visual and vestibular motion perception (see Angelaki, Gu, and Deangelis (2011) for a discussion).

Muscle spindle feedback (CCR) stabilizes the head on the torso. The CCR also proved essential for stabilization of the individual intervertebral joints and to prevent neck buckling. Without CCR, static stability could not be achieved, resulting in excessive static flexion or extension of the individual neck joints and the entire neck (Happee et al., 2017). Without VCR, the neck model could be stabilized provided CCR gains were adapted and provided a reasonable fit for horizontal seat translation conditions (AP and LAT). This concurs with observations in vestibular loss patients where "there are no dramatic differences between patients and controls" in conditions similar to APEC (Keshner, 2003).

Neck muscle cocontraction (G_{cc}) was estimated to be up to 1% of maximal muscle activation. Cocontraction contributed to head-on-trunk stabilization up to 1 Hz but was not essential for dynamic and static stabilization. This highlights a minor contribution of neck muscle cocontraction in natural stabilization conditions. It shall be noted that Keshner (2000) found that both younger (20−40 years) and older (65−88 years) subjects showed effective cocontraction when asked to stiffen their necks, while the older subjects also showed effective cocontraction with mental arithmetic and relax tasks. As discussed in the results section, raised cocontraction may also explain higher STHT in the experimental corridor from the study by Paddan and Griffin (1998) in Fig. 19.3.

Experimental studies have shown the ability of the central nervous system (CNS) to modulate neck afferent feedback in response to changing external environments (Fard, Ishihara, & Inooka, 2004; Gillies, Broaddus, Stenger, & Taylor, 1998; Goldberg & Peterson, 1986; Keshner et al., 1999; Liang & Chiang, 2008; Reynolds, Blum, & Gdowski, 2008). We demonstrated modulation of neck afferent feedback with the frequency bandwidth of anterior−posterior trunk perturbations (Forbes, de Bruijn et al., 2013), with modest effects of the presence of vision. The neck model enabled the estimation of postural control parameters for these conditions (Happee et al., 2017). Control strategies used during low-bandwidth perturbations most effectively reduced head rotation and head relative displacement up to 3 Hz, while control strategies used reduced head global translation between 1 and 4 Hz during high bandwidth perturbations. This indicates a shift from minimizing head-on-trunk rotation and translation during low-bandwidth perturbations to minimizing head-in-space translation during high-bandwidth perturbations. This modulation of control may well be beneficial in terms of comfort, limiting the transfer of 1−4 Hz horizontal seat motions to the head, where comfort standards for whole-body vibration attribute considerable weight to these frequencies (ISO-2631-1, 1997).

Experiments testing the complete spine were used to study and model lumbar stabilization. The developed one DOF lumbar models separate stabilizing contributions of intrinsic stiffness and damping (including muscle cocontraction) and muscle feedback (length, velocity, and acceleration). Where the neck model separates intrinsic properties into nonlinear passive stiffness and damping, cocontraction, and gravity, the lumbar models lump all intrinsic contributions in a linear stiffness and damping, which may be separated in future models. The model parameters allowed us to estimate the relative contributions of intrinsic and reflexive stabilization and showed intrinsic contributions, similar to or larger than reflexive contributions in lumbar stabilization with horizontal perturbations to the trunk or pelvis. Experiments with a rotating pelvis showed relevant contributions of vestibular and visual feedback, which are more effective to minimize head than trunk rotation. This is even more striking when we compare platform pitch experiments with unrestrained torso to similar experiments with the torso supported. With unrestrained torso, head rotations are below 10% of platform rotations up to 10 Hz (Fig. 19.14), illustrating effective head-in-space control through coordinated control of the entire spine. With supported torso, head rotations exceed 30% (Fig. 19.7), illustrating a limited ability of the neck to deal with torso pitch rotations. Fig. 19.6 shows similar results in torso roll, while Fig. 19.8 shows that the neck can effectively compensate for torso twist. A next step will be to use such data to model vestibular and visual contributions to stabilization of the full spine, capturing combined torso and head stabilization.

4.2 Motion comfort

This manuscript presents experimental and modeling efforts to investigate and predict STHT, applying mechanical perturbations to seated subjects and measuring torso and head motion to investigate postural stabilization. To use such models in the vehicle and seat design process, a full-body biomechanical human model is needed. An early passive version of the neck model, as presented in this manuscript, was integrated in a full-body model (Happee et al., 1998; Happee & Loczi, 1999), see Fig. 19.15, and validated for vertical vibration transmission on rigid and compliant seats (Happee et al., 2000; Verver et al., 2005). Integrating the new neck model with recently developed lumbar, hip, and arm stabilizing models (Broos & Meijer, 2016; Meijer et al., 2013) will provide a full-body model with stabilizing controllers at the essential joints.

FIGURE 19.15 Full-body biomechanical human model interacting with a car seat, where seat and soft-tissue compliance is modeled using stress-penetration curves.

Such biomechanical models may allow evaluation of the interaction between the human and the seat and other body supports. This may allow predictions of comfort and motion sickness using established comfort norms (British Standards Institution, 1987; ISO-2631-1, 1997), which relate frequency-weighted accelerations measured at the seat surface to motion sickness and vibration discomfort. While these norms do correlate to comfort, a better understanding and prediction of motion comfort may be achieved by measuring and modeling head motion and visual and vestibular motion perception. Head motion can serve as input to motion sickness models as published by Bles, Bos, De Graaf, Groen, and Wertheim (1998) and Oman (1990). Further experimental and modeling efforts may aim to capture sensory integration of visual and vestibular motion perception to better predict motion sickness (Bles et al., 1998). In future studies, we aim to measure and model STHT and comfort, in particular, for users of automated vehicles performing nondriving tasks with eyes off road. Where active drivers typically stabilize head and eyes in space, users of automated vehicles may choose to stabilize body and head relative to the vehicle and personal devices. Hence vestibular feedback will be less effective, and visual and muscular feedback may dominate. Such changes in control strategy can be effectively investigated and explained using postural models as presented in this manuscript.

The available validation data displayed substantial variations between studies, between subjects, and even within subjects. Within-subject variations may derive from instruction sets, as evidenced comparing the instructions MA and NV (both without vision) in Figs. 19.7 and 19.8. In line with the ecological theory (Riccio & Stoffregen, 1991), between-subject differences may relate to the individual motion sickness susceptibility.

As suggested previously, biomechanical full-body human models can be used to design seats such that STHT is reduced at frequencies associated with motion sickness and general discomfort. Seats may be modeled in various levels of detail including finite elements if needed. However, to design the control strategies of automated vehicles, detailed seat and human models may not be needed. Instead descriptive models can be developed, for instance, using 6DOF transfer functions as shown in Fig. 19.9. The STHT can be described by two 6DOF functions in series capturing transmission from seat to T1 and from T1 to head. Biomechanical models can be used to estimate the human postural control strategies and feedback parameters using experimental data for specific driving conditions and seats. 6DOF transfer functions derived from the biomechanical model can then extrapolate STHT to similar conditions for a wider range of frequencies and motion directions. Head motion−based models predicting motion sickness and general (dis)comfort can be used to optimize vehicle control in terms of path planning, path following, and active suspension.

Acknowledgments

Research on comfort of automated driving has been performed as part of the German-Dutch Interreg project Interregional Automated Transport (I-AT) http://www.euregio.org/action/projects/item/126/i-at—interregional-automated-transport. Earlier research by the authors on neck and lumbar stabilization as reviewed in this manuscript has been performed as part of the Dutch NWO projects 10736 (Torticollis) and 10732 (QDISC).

References

Almeida, J., Fraga, F., Silva, M., & Silva-Carvalho, L. (2009). Feedback control of the head-neck complex for nonimpact scenarios using multibody dynamics. *Multibody System Dynamics, 21*(4), 395–416. https://doi.org/10.1007/s11044-009-9148-4.

Angelaki, D. E., Gu, Y., & Deangelis, G. C. (2011). Visual and vestibular cue integration for heading perception in extrastriate visual cortex. *Journal of Physiology, 589*(Pt 4), 825–833. https://doi.org/10.1113/jphysiol.2010.194720.

Bär, M. (2014). *Vorausschauende Fahrwerk Regelung zur Reduktion der auf die Insassen wirkende Querbeschleunigung* (PhD). RWTH Aachen. Retrieved from https://www.ika.rwth-aachen.de/de/forschung/publikationen/dissertationen/129-dissertations/43-16814-b%C3%A4r-vorausschauende-fahwerkregelung.html.

Bellem, H., Schönenberg, T., Krems, J. F., & Schrauf, M. (2016). Objective metrics of comfort: Developing a driving style for highly automated vehicles. *Transportation Research Part F: Traffic Psychology and Behaviour, 41*, 45–54. https://doi.org/10.1016/j.trf.2016.05.005.

Bertolini, G., & Straumann, D. (2016). Moving in a moving world: A review on vestibular motion sickness. *Frontiers in Neurology, 7*(FEB). https://doi.org/10.3389/fneur.2016.00014.

Bles, W., Bos, J. E., De Graaf, B., Groen, E., & Wertheim, A. H. (1998). Motion sickness: Only one provocative conflict? *Brain Research Bulletin, 47*(5), 481–487. https://doi.org/10.1016/S0361-9230(98)00115-4.

Borst, J., Forbes, P. A., Happee, R., & Veeger, H. E. J. (2011). Muscle parameters for musculoskeletal modelling of the human neck. *Clinical Biomechanics, 26*(4), 343–351. https://doi.org/10.1016/j.clinbiomech.2010.11.019. S0268-0033(10)00313-X [pii].

British Standards Institution. (1987). *British standard guide to measurement and evaluation of human exposure to whole-body mechanical vibration and repeated shock (BS 6841)*. https://shop.bsigroup.com/ProductDetail/?pid=000000000000171912.

Brolin, K., Hedenstierna, S., Halldin, P., Bass, C., & Alem, N. (2008). The importance of muscle tension on the outcome of impacts with a major vertical component. *International Journal of Crashworthiness, 13*(5), 487–498. https://doi.org/10.1080/13588260802215510.

Broos, J., & Meijer, R. (2016). Simulation method for whiplash injury prediction using an active human model. In *Paper presented at the 2016 IRCOBI conference proceedings - international research council on the biomechanics of injury*.

de Bruijn, E., van der Helm, F. C. T., & Happee, R. (2015). Analysis of isometric cervical strength with a nonlinear musculoskeletal model with 48 degrees of freedom. *Multibody System Dynamics, 36*(4), 339–362. https://doi.org/10.1007/s11044-015-9461-z.

Chancey, V. C., Nightingale, R. W., Van Ee, C. A., Knaub, K. E., & Myers, B. S. (2003). Improved estimation of human neck tensile tolerance: Reducing the range of reported tolerance using anthropometrically correct muscles and optimized physiologic initial conditions. *Stapp Car Crash Journal, 47*, 135–153, 2003-22-0008 [pii].

Cullen, K. E. (2012). The vestibular system: Multimodal integration and encoding of self-motion for motor control. *Trends in Neurosciences, 35*(3), 185–196. https://doi.org/10.1016/j.tins.2011.12.001.

van Dieën, J. H., van Drunen, P., & Happee, R. (2017). Sensory contributions to stabilization of trunk posture in the sagittal plane. *Journal of Biomechanics*. https://doi.org/10.1016/j.jbiomech.2017.07.016.

Diels, C., & Bos, J. E. (2016). Self-driving carsickness. *Applied Ergonomics, 53*, 374–382. https://doi.org/10.1016/j.apergo.2015.09.009.

van Drunen, P., Koumans, Y., van der Helm, F. C. T., van Dieën, J. H., & Happee, R. (2015). Modulation of intrinsic and reflexive contributions to low-back stabilization due to vision, task instruction and perturbation bandwidth. *Experimental Brain Research, 233*(3). https://doi.org/10.1007/s00221-014-4151-2.

van Drunen, P., Maaswinkel, E., van der Helm, F. C. T., van Dieën, J. H., & Happee, R. (2013). Identifying intrinsic and reflexive contributions to low-back stabilization. *Journal of Biomechanics, 46*(8), 1440–1446. https://doi.org/10.1016/j.jbiomech.2013.03.007.

van Drunen, P., Maaswinkel, E., van der Helm, F. C. T., van Dieën, J. H., & Happee, R. (2014). Corrigendum to Identifying intrinsic and reflexive contributions to low-back stabilization [J. Biomech. 46(8) (2013) 1440-1446]. *Journal of Biomechanics, 47*(8), 1928–1929. https://doi.org/10.1016/j.jbiomech.2014.03.013.

van Drunen, P., van der Helm, F. C. T., van Dieën, J. H., & Happee, R. (2016). Trunk stabilization during sagittal pelvic tilt: From trunk-on-pelvis to trunk-in-space due to vestibular and visual feedback. *Journal of Neurophysiology, 115*(3), 1381–1388. https://doi.org/10.1152/jn.00867.2015.

van Ee, C. A., Nightingale, R. W., Camacho, D. L., Chancey, V. C., Knaub, K. E., Sun, E. A., & Myers, B. S. (2000). Tensile properties of the human muscular and ligamentous cervical spine. *Stapp Car Crash Journal, 44*, 85–102, 2000-01-SC07 [pii].

Ewing, C., & Thomas, D. (1972). *Human head and neck response to impact acceleration (NAMRL monograph 21)*. Retrieved from http://www.dtic.mil/dtic/tr/fulltext/u2/747988.pdf.

Ewing, C., Thomas, D., Lustick, L., Muzzy, W., Willems, G., & Majewski, P. (1976). The effect of duration, rate of onset, and peak sled acceleration on the dynamic response of the human head and neck. In *Paper presented at the 20th stapp car crash conference, Dearborn, MI; United States*.

Ewing, C. L., Thomas, D. J., Patrick, L. M., Beeler, G. W., & Smith, M. J. (1969). *Living human dynamic response to —gx impact acceleration II—accelerations measured on the head and neck*. https://doi.org/10.4271/690817.

Fard, M. A., Ishihara, T., & Inooka, H. (2003). Dynamics of the head-neck complex in response to the trunk horizontal vibration: Modeling and identification. *Journal of Biomechanical Engineering, 125*(4), 533–539.

Fard, M. A., Ishihara, T., & Inooka, H. (2004). Identification of the head-neck complex in response to trunk horizontal vibration. *Biological Cybernetics, 90*(6), 418–426. https://doi.org/10.1007/s00422-004-0489-z.

Fernandez, C., Goldberg, J. M., & Abend, W. K. (1972). Response to static tilts of peripheral neurons innervating otolith organs of the squirrel monkey. *Journal of Neurophysiology, 35*(6), 978–987.

Festner, M., Baumann, H., & Schramm, D. (2016). Der Einfluss fahrfremder Tätigkeiten und Manöverlängsdynamik auf die Komfort- und Sicherheitswahrnehmung beim hochautomatisierten Fahren. In *Paper presented at the 32. VDI/VW-Gemeinschaftstagung Fahrerassistenzsysteme und automatisiertes Fahren, Wolfsburg*. https://www.researchgate.net/publication/310802392_Der_Einfluss_fahrfremder_Tatigkeiten_und_Manoverlangsdynamik_auf_die_Komfort-_und_Sicherheitswahrnehmung_beim_hochautomatisierten_Fahren.

Forbes, P. A. (2014). *Heads up − sensorimotor control of the head-neck system*. PhD thesis. (PhD Thesis). Delft University of Technology. Retrieved from http://repository.tudelft.nl/assets/uuid:dcefd6fd-b198-47da-8862-549e94003d9c/HEADS_UP_-_Sensorimotor_control_of_the_head-neck_system_-_Patrick_Alan_Forbes.pdf.

Forbes, P. A., Dakin, C. J., Vardy, A. N., Happee, R., Siegmund, G. P., Schouten, A. C., & Blouin, J. S. (2013a). Frequency response of vestibular reflexes in neck, back, and lower limb muscles. *Journal of Neurophysiology, 110*(8), 1869−1881. https://doi.org/10.1152/jn.00196.2013.

Forbes, P. A., de Bruijn, E., Schouten, A. C., van der Helm, F. C. T., & Happee, R. (2013b). Dependency of human neck reflex responses on the bandwidth of pseudorandom anterior-posterior torso perturbations. *Experimental Brain Research, 226*(1), 1−14. https://doi.org/10.1007/s00221-012-3388-x.

Gillies, G. T., Broaddus, W. C., Stenger, J. M., & Taylor, A. G. (1998). A biomechanical model of the craniomandibular complex and cervical spine based on the inverted pendulum. *Journal of Medical Engineering & Technology, 22*(6), 263−269.

Goldberg, J. M., & Cullen, K. E. (2011). Vestibular control of the head: Possible functions of the vestibulocollic reflex. *Experimental Brain Research, 210*(3−4), 331−345. https://doi.org/10.1007/s00221-011-2611-5.

Goldberg, J., & Peterson, B. W. (1986). Reflex and mechanical contributions to head stabilization in alert cats. *Journal of Neurophysiology, 56*(3), 857−875.

Happee, R., de Bruijn, E., Forbes, P. A., & van der Helm, F. C. T. (2017). Dynamic head-neck stabilization and modulation with perturbation bandwidth investigated using a multisegment neuromuscular model. *Journal of Biomechanics, 58*, 203−211. https://doi.org/10.1016/j.jbiomech.2017.05.005.

Happee, R., de Vlugt, E., & van Vliet, B. (2014). Nonlinear 2D arm dynamics in response to continuous and pulse-shaped force perturbations. *Experimental Brain Research, 233*(1), 39−52. https://doi.org/10.1007/s00221-014-4083-x.

Happee, R., Hoofman, M., van den Kroonenberg, A. J., Morsink, P., & Wismans, J. (1998). A mathematical human body model for frontal and rearward seated automotive impact loading. *SAE Technical Papers*. https://doi.org/10.4271/983150.

Happee, R., & Loczi, J. (1999). Human seat interaction simulation using RAMSIS and the dynamic simulation program MADYMO. *SAE Technical Papers*. https://doi.org/10.4271/1999-01-3737.

Happee, R., Verver, M. M., & de Lange, R. (2000). Simulation of human seated postures and dynamic seat interaction in impact conditions. *Proceedings of the Human Factors and Ergonomics Society - Annual Meeting, 44*(38), 861−864. https://doi.org/10.1177/154193120004403849.

Hedenstierna, S. (2008). *3D finite element modeling of cervical musculature and its effect on neck injury prevention*. PhD thesis. Stockholm: KTH. Retrieved from http://urn.kb.se/resolve?urn=urn:nbn:se:kth:diva-9503.

Hedenstierna, S., & Halldin, P. (2008). How does a three-dimensional continuum muscle model affect the kinematics and muscle strains of a finite element neck model compared to a discrete muscle model in rear-end, frontal, and lateral impacts. *Spine, 33*(8), E236−E245. https://doi.org/10.1097/BRS.0b013e31816b8812.

Hedenstierna, S., Halldin, P., & Brolin, K. (2008). Evaluation of a combination of continuum and truss finite elements in a model of passive and active muscle tissue. *Computer Methods in Biomechanics and Biomedical Engineering, 11*(6), 627−639. https://doi.org/10.1080/17474230802312516.

van der Horst, M. J. (2002). *Human head and neck response in frontal, lateral, and impact loading*. Eindhoven: Technical University of Eindhoven. PhD thesis. (PhD Thesis).

van der Horst, M. J., Bovendeerd, P. H. M., Happee, R., & Wismans, J. S. H. M. K.,H. (2001). Simulation of rear end impact with a full body human model with a detailed neck: Role of passive muscle properties and initial seating posture. In *Paper presented at the international technical conference on the enhanced safety of vehicles*. Amsterdam: ESV).

van der Horst, M. J., Thunnissen, J. G. M., Happee, R., & van Haaster, R. M. H. P. (November 13-14, 1997). The influence of muscle activity on head-neck response during impact. In *Paper presented at the Stapp car crash conference proceedings*. Orlando, Florida: SAE).

ISO-2631-1. (1997). *Mechanical vibration and shock: Evaluation of human exposure to whole-body vibration*.

de Jager, M. K. J. (1996). *Mathematical head-neck models for acceleration impacts*. PhD thesis. (PhD Thesis). University of Eindhoven. Retrieved from https://pure.tue.nl/ws/files/3731961/460661.pdf.

Kearney, R. E., Stein, R. B., & Parameswaran, L. (1997). Identification of intrinsic and reflex contributions to human ankle stiffness dynamics. *IEEE Transactions on Biomedical Engineering, 44*(6), 493−504.

Keshner, E. A. (2000). Modulating active stiffness affects head stabilizing strategies in young and elderly adults during trunk rotations in the vertical plane. *Gait & Posture, 11*(1), 1−11.

Keshner, E. A. (2003). Head-trunk coordination during linear anterior-posterior translations. *Journal of Neurophysiology, 89*(4), 1891−1901. https://doi.org/10.1152/jn.00836.2001.

Keshner, E. A. (2009). Vestibulocollic and cervicocollic control. In M. D. Binder, N. Jirokawa, & U. Windhorst (Eds.), *Encyclopedia of neuroscience* (pp. 4222−4224). Berlin, Heidelberg: Springer-Verlag.

Keshner, E. A., Cromwell, R. L., & Peterson, B. W. (1995). Mechanisms controlling human head stabilization. II. Head-neck dynamics during random rotations in the vertical plane. *Journal of Neurophysiology, 73*(6), 2302−2312.

Keshner, E. A., Hain, T. C., & Chen, K. J. (1999). Predicting control mechanisms for human head stabilization by altering the passive mechanics. *Journal of Vestibular Research, 9*(6), 423−434.

Keshner, E. A., & Peterson, B. W. (1995). Mechanisms controlling human head stabilization. I. Head-neck dynamics during random rotations in the horizontal plane. *Journal of Neurophysiology, 73*(6), 2293−2301.

Kyriakidis, M., Happee, R., & De Winter, J. C. F. (2015). Public opinion on automated driving: Results of an international questionnaire among 5000 respondents. *Transportation Research Part F: Traffic Psychology and Behaviour, 32*, 127−140. https://doi.org/10.1016/j.trf.2015.04.014.

Lange, A. M. M., Siedersberger, K. H., & Bengler, K. (2014). *Automatisiertes Fahren − So komfortabel wie öglich, so dynamisch wie nötig. Vestibuläre Zustandsruckmeldung beim automatisierten Fahren*. Paper presented at the VDI Wissensforum 2013.

Liang, C. C., & Chiang, C. F. (2008). Modeling of a seated human body exposed to vertical vibrations in various automotive postures. *Industrial Health, 46*(2), 125−137. https://doi.org/10.2486/indhealth.46.125.

MADYMO. (2012). *Human body models manual*. Version 7.3). Rijswijk, The Netherlands. Retrieved from www.tassinternational.com www.tassinternational.com.

Mathworks. (2012). *Matlab R2012b natick*. USA. Retrieved from www.mathworks.com.

Meijer, R., Broos, J., Elrofai, H., De Bruijn, E., Forbes, P., & Happee, R. (2013). Modelling of bracing in a multi-body active human model. In *Paper presented at the 2013 IRCOBI conference proceedings - international research council on the biomechanics of injury*.

Meyer, F., Bourdet, N., Gunzel, K., & Willinger, R. (2013). Development and validation of a coupled head-neck FEM-application to whiplash injury criteria investigation. *International Journal of Crashworthiness, 18*(1), 40−63. https://doi.org/10.1080/13588265.2012.732293.

Meyer, F., Bourdet, N., Willinger, R., Legall, F., & Deck, C. (2004). Finite element modelling of the human head-neck: Modal analysis and validation in the frequency domain. *International Journal of Crashworthiness, 9*(5), 535−545. https://doi.org/10.1533/ijcr.2004.0309.

Meyer, F., & Willinger, R. (2009). Three-year-old child head-neck finite element modelling: Simulation of the interaction with airbag in frontal and side impact. *International Journal of Vehicle Safety, 4*(4), 285−299. https://doi.org/10.1504/IJVS.2009.032757.

Mirbagheri, M. M., Barbeau, H., & Kearney, R. E. (2000). Intrinsic and reflex contributions to human ankle stiffness: Variation with activation level and position. *Experimental Brain Research, 135*(4), 423−436.

Oman, C. M. (1990). Motion sickness: A synthesis and evaluation of the sensory conflict theory. *Canadian Journal of Physiology and Pharmacology, 68*(2), 294−303. https://doi.org/10.1139/y90-044.

Östh, J., Brolin, K., & Bråse, D. (2015). A human body model with active muscles for simulation of pretensioned restraints in autonomous braking interventions. *Traffic Injury Prevention, 16*(3), 304−313. https://doi.org/10.1080/15389588.2014.931949.

Östh, J., Eliasson, E., Happee, R., & Brolin, K. (2014). A method to model anticipatory postural control in driver braking events. *Gait & Posture, 40*(4), 664−669. https://doi.org/10.1016/j.gaitpost.2014.07.021.

Östh, J., Mendoza-Vazquez, M., Svensson, M. Y., Linder, A., & Brolin, K. (2016). Development of a 50th percentile female human body model. In *Paper presented at the 2016 IRCOBI conference proceedings - international research council on the biomechanics of injury*.

Paddan, G. S., & Griffin, M. J. (1988). The transmission of translational seat vibration to the head-I. Vertical seat vibration. *Journal of Biomechanics, 21*(3), 191−197. https://doi.org/10.1016/0021-9290(88)90169-8.

Paddan, G. S., & Griffin, M. J. (1998). A review of the transmission of translational seat vibration to the head. *Journal of Sound and Vibration, 215*(4), 863−882.

Peng, G. C. Y., Hain, T. C., & Peterson, B. W. (1996). A dynamical model for reflex activated head movements in the horizontal plane. *Biological Cybernetics, 75*(4), 309−319. https://doi.org/10.1007/s004220050297.

Peng, G. C. Y., Hain, T. C., & Peterson, B. W. (1997). How is the head held up? Modeling mechanisms for head stability in the sagittal plane. In *Paper presented at the proceedings of the 18th annual international conference of the IEEE engineering in medicine and biology society* (Vol. 18, pp. 1−5).

Peng, G. C., Hain, T. C., & Peterson, B. W. (1999). Predicting vestibular, proprioceptive, and biomechanical control strategies in normal and pathological head movements. *IEEE Transactions on Biomedical Engineering, 46*(11), 1269−1280. https://doi.org/10.1109/10.797986.

Reynolds, J. S., Blum, D., & Gdowski, G. T. (2008). Reweighting sensory signals to maintain head stability: Adaptive properties of the cervicocollic reflex. *Journal of Neurophysiology, 99*(6), 3123−3135. https://doi.org/10.1152/jn.00793.2007.

Riccio, G. E., & Stoffregen, T. A. (1991). An ecological theory of motion sickness and postural instability. *Ecological Psychology, 3*(3), 195−240. https://doi.org/10.1207/s15326969eco0303_2.

Schneider, A. D., Jamali, M., Carriot, J., Chacron, M. J., & Cullen, K. E. (2015). The increased sensitivity of irregular peripheral canal and otolith vestibular afferents optimizes their encoding of natural stimuli. *Journal of Neuroscience, 35*(14), 5522−5536. https://doi.org/10.1523/JNEUROSCI.3841-14.2015.

Shyrokau, B., Wang, D., Savitski, D., Hoepping, K., & Ivanov, V. (2015). Vehicle motion control with subsystem prioritization. *Mechatronics, 30*, 297−315. https://doi.org/10.1016/j.mechatronics.2014.11.004.

Stemper, B. D., Yoganandan, N., & Pintar, F. A. (2004). Validation of a head-neck computer model for whiplash simulation. *Medical, & Biological Engineering & Computing, 42*(3), 333−338. https://doi.org/10.1007/bf02344708.

Stensdotter, A. K., Dinhoffpedersen, M., Meisingset, I., Vasseljen, O., & Stavdahl, Ø. (2016). Mechanisms controlling human head stabilization during random rotational perturbations in the horizontal plane revisited. *Physiological Reports, 4*(10). https://doi.org/10.14814/phy2.12745.

Verver, M. M., Dalenoort, A. M., & Mooi, H. G. (2005). Spinal muscle modelling for prediction of human resonance behaviour in vertical vibrations by numerical simulations. *SAE Technical Papers,* 01, 2711.

de Vlugt, E., Schouten, A. C., & van der Helm, F. C. T. (2006). Quantification of intrinsic and reflexive properties during multijoint arm posture. *Journal of Neuroscience Methods, 155*(2), 328−349. https://doi.org/10.1016/j.jneumeth.2006.01.022.

Wittek, A., Kajzer, J., & Haug, E. (2000). Hill-type muscle model for analysis of mechanical effect of muscle tension on the human body response in a car collision using an explicit finite element code. *JSME International Journal - Series A: Solid Mechanics and Material Engineering, 43*(1), 8−18.

Yoganandan, N., Pintar, F. A., & Cusick, J. F. (2002). Biomechanical analyses of whiplash injuries using an experimental model. *Accident Analysis & Prevention, 34*(5), 663−671. https://doi.org/10.1016/s0001-4575(01)00066-5.